Biphasic Kinetics of Activation and Signaling for PAR1 and PAR4 Thrombin Receptors in Platelets†

Lidija Covic, Amy L. Gresser, and Athan Kuliopulos*

Molecular Cardiology Research Institute, Division of Hematology/Oncology, New England Medical Center, and Departments of Medicine and Biochemistry, Tufts University School of Medicine, Boston, Massachusetts 02111

Received November 24, 1999; Revised Manuscript Received February 8, 2000

ABSTRACT: Thrombin activates platelets in an ordered sequence of events that includes shape change, increase in cytoplasmic Ca^{2+}, activation of the αIIbβ3 integrin, granule secretion, aggregation, and formation of a stable hemostatic plug. Activation of this process has also been implicated in the pathogenesis of atherosclerosis, stroke, and thrombosis. There are two identified thrombin-activated receptors on the surface of human platelets. PAR1 is a high-affinity thrombin receptor, and PAR4 is a low apparent affinity thrombin receptor of uncertain function. The goal of these studies is to determine the kinetics of thrombin activation of PAR1 and PAR4 and to relate the individual inputs from each receptor to platelet Ca^{2+} signaling, secondary autocrine stimulation, and aggregation. Using a combination of PAR-specific peptide ligands and anti-PAR1 reagents, we separated the biphasic thrombin Ca^{2+} response of platelets into two discrete components—a rapid spike response caused by PAR1, followed by a slower prolonged response from PAR4. Despite having a 20−70-fold slower rate of activation, PAR4 produces the majority of the integrated Ca^{2+} signal that is sustained by the continuous presence of catalytically active thrombin. Surprisingly, PAR4 activation is much more effective than PAR1 activation in mounting secondary autocrine Ca^{2+} signals from secreted ADP. The strong ADP response due to activated PAR4, however, requires prior activation of PAR1 as would normally occur during treatment of platelets with thrombin. Thus, the late signal generated by activated PAR4 is not redundant with the early signal from PAR1 and instead serves to greatly extend the high intracellular Ca^{2+} levels that support the late phase of the platelet aggregation process.

The majority of seven transmembrane G protein-coupled receptors respond to freely diffusible ligands. Receptors that operate under conditions of high external flow, such as those located on the surface of platelets, are not likely to experience sustained high local ligand concentration levels at or above the dissociation constants for their cognate ligand. The subclass of protease-activated receptors (PARs)[1] has provided a unique solution to this problem by incorporating the ligand into their N-terminal extracellular domains (*1*). The protease receptors are activated by proteolytic cleavage at a specific site to unmask a new amino terminus that acts as a tethered ligand (*2*). The first protease receptor to be discovered was the PAR1 thrombin receptor (*2, 3*). Three additional protease-activated receptors have since been identified: PAR2, PAR3, and PAR4 (*4*−*7*). PAR3 is likely to be a major thrombin receptor in mouse platelets but is not expressed on human platelets (*8*). PAR2 is activated by trypsin/tryptase but not by thrombin (*4*), and PAR4 is activated by thrombin and trypsin and is expressed on both mouse and human platelets (*6*, *9*).

A critical issue to be addressed is what is the physiological role of PAR4 in platelet thrombin responses? Recent experiments demonstrated that activation of either PAR1 or PAR4 with synthetic peptide ligands is sufficient to cause granule secretion and aggregation (*9*). Simultaneous blockade of PAR1 and PAR4 with antibodies eliminated granule secretion and aggregation to thrombin, implying that these two receptors account for all of the thrombin responses on platelets. Another report (*10*) suggested that PAR1 is the primary thrombin receptor and that PAR4 provides modest stimulation of platelets comparable to weak agonists such as ADP or epinephrine. Nonetheless, a major clue that PAR4 might serve an important auxiliary function in human platelets is that the PAR1-specific ligand, SFLLRN, elicits a less robust subset of responses as compared to thrombin (*2, 11*−*13*). These differences are especially striking when one compares the Ca^{2+} responses (*12, 13*). The much larger intracellular Ca^{2+} signal generated by treatment with thrombin versus SFLLRN (*13*) has been variously attributed to αIIbβ3-mediated thromboxane synthesis and non-PAR1 thrombin receptors such as GPIb (*14*). Thrombin and SFLLRN activation of platelet thrombin receptors stimulates rapid and transient production of inositol triphosphate (IP_3) and diacylglycerol whose peak concentrations coincide with the $[Ca^{2+}]_{max}$ (*11, 15*). This early process requires G_q because

† This work was supported by National Institutes of Health Grant R01HL57905-01, and by Scholar Awards from the PEW Charitable Trusts and the American Society of Hematology (to A.K.).

* To whom correspondence should be addressed at the Molecular Cardiology Research Institute, Division of Hematology/Oncology, New England Medical Center, Box 832, 750 Washington St., Boston, MA 02111. Fax: (617) 636-4833; E-mail: akuliopu@opal.tufts.edu.

[1] Abbreviations: PAR, protease-activated receptor; IP_3, inositol triphosphate; CMP, calcium mobilizing-potency; T, thrombin; H, hirudin.

10.1021/bi9927078 CCC: $19.00
Published on Web 04/09/2000

platelets from G_q (-/-) mice that completely lack thrombin-dependent phosphoinositide and Ca^{2+} responses cannot aggregate (*16*). Likewise, humans deficient in G_q have impaired thrombin-induced IP_3 formation and Ca^{2+} mobilization in platelets and suffer from a bleeding diathesis (*17*). Ca^{2+} mobilization derives from IP_3-dependent intracellular store-release from the dense tubular system and Ca^{2+} entry from extracellular sources (*18*). The late phase of the thrombin-dependent Ca^{2+} response has been ascribed to activation of plasma membrane Ca^{2+} channels (*19*) and is not strictly dependent on secondary ADP or thromboxane release from platelet granules (*13*). The identities of the Ca^{2+} channels on the platelet plasma membrane are currently unknown, but may be controlled in part by phosphatidylinositol 3,4,5-triphosphate (PIP_3) generated by PI3-kinase (*20*, *21*).

The intracellular Ca^{2+} signal, in turn, controls many of the events leading to platelet aggregation. Platelet−platelet aggregation requires the translocation of cytosolic proteins to the actin cytoskeleton and formation of the αIIbβ3-associated focal adhesion complex (*22*). αIIbβ3 forms a link between the actin cytoskeleton inside the platelet and the extracellular fibrin matrix to promote irreversible platelet aggregation (*23*). Several of the cytoskeletal-reorganizing proteins such as gelsolin (*24*) and calpain (*25*, *26*) require micromolar Ca^{2+} concentrations that are achieved during the late phase of platelet activation. The activity of the Ca^{2+}-dependent protease calpain plays a role in platelet granule secretion, aggregation, and spreading (*27*, *28*). The high intracellular Ca^{2+} levels also modulate the activity of the calmodulin-dependent myosin light-chain kinase which controls the myosin-based movement of actin (*29*). Actin−myosin contraction of the adhesion foci eventually leads to fibrin clot retraction, hemostasis, and wound closure to complete the late phase of platelet activation.

Here, we determine when the PAR1 and PAR4 thrombin receptors are operational during defined periods along the time course of platelet activation. We demonstrate that there are two separate thrombin receptor-dependent Ca^{2+} transients: a very early spike response from PAR1, followed by a prolonged Ca^{2+} signal that arises from PAR4 receptors that are slowly activated by thrombin. Unlike PAR1, PAR4 is a very strong stimulator of the autocrine Ca^{2+} response from secreted ADP. Thus, PAR1 and PAR4 do not produce redundant signals during platelet activation but instead complement each other by evoking two distinct waves of intracellular Ca^{2+}.

MATERIALS AND METHODS

Materials. Human thrombin (3000 NIH units/mg) was purchased from Haematologic Technologies Inc. (Essex Junction, VT). Recombinant hirudin was from Calbiochem (La Jolla, CA), and apyrase and RGDS were from Sigma (St. Louis, MO). The peptide ligands SFLLRN, GYPGQV, and GYPGKF were synthesized with C-terminal amides and were >95% pure. The BMS-88 compound (*30*), *trans*-cinnamoyl-F(f)-F(Gn)L-R-Orn(propionyl)-NH_2, was synthesized by Star Biochemicals (Torrance, CA). The SFLLR-Ab (PAR1) rabbit polyclonal antibody is directed against the human PAR1 ligand region residues S_{42}FLLRNPNDK-YEPF$_{55}$C and purified as described (*31*, *32*). The E2-Ab rabbit polyclonal antibody was raised against the first extracellular loop of human PAR1, residues S_{164}−A_{181}. Antibodies were purified from rabbit antiserum using peptide−Sepharose 4B affinity columns (*32*).

Cytosolic Calcium Measurements. Cytosolic calcium measurements were carried out in gel-filtered human platelets and COS7 cells transiently transfected with PAR1 (*32*). COS7 cells were detached from flasks by incubation at 37 °C, 5% CO_2, with 1.5 mM EDTA in PBS for 5−15 min. Detached cells were resuspended and washed in KRB buffer (118 mM NaCl, 1 mM $CaCl_2$, 1 mM KH_2PO_4, 1.2 mM $MgSO_4 \cdot 7H_2O$, 1 mg/mL BSA, 0.72 mg/mL dextrose, 20 mM HEPES, pH 7.2). Blood was drawn from healthy volunteer donors with an 18 gauge needle into a 30 mL syringe containing 3 mL of 4% sodium citrate (0.4% v/v final). Platelets were isolated by gel filtration chromatography using Sepharose 2B (Pharmacia) in modified PIPES buffer (*33*), leaving out inhibitors of platelet function (i.e., aspirin or prostaglandins). Platelets eluted from the gel filtration column were counted on a Coulter counter and adjusted to $1.5 \times 10^5/\mu$L in KRB buffer. COS7 cells were collected by centrifugation at 700*g* for 5 min and adjusted to 1×10^6 cells/mL in KRB buffer. Cells were loaded with 2.5 μM fura-2/AM (Molecular Probes) for 30 min at 37 °C, 5% CO_2 with gentle rotation for platelets and more vigorous rotation (150 rpm) for COS7 cells. After thorough washing in KRB buffer, COS7 cells were resuspended in fresh KRB buffer at 1×10^6 cells/mL; platelets at 1.5×10^8 cells/mL. Fluorescence experiments were performed at 25 °C. The fluorescence emission of fura-2 ($I_{340/380}$) was recorded at 510 nm with dual excitation at 340 and 380 nm in a Perkin-Elmer LS50B spectrofluorometer. Measurements of platelet intracellular Ca^{2+} ($[Ca^{2+}]_i$) were performed without stirring; COS7 cells were stirred at 300 rpm with a magnetic microstir bar. At the end of each experiment, the Ca^{2+} concentration was calibrated by the addition of 12 mM EGTA followed by 0.38 mM digitonin plus 15 mM $CaCl_2$ using a K_d of 224 nM for fura-2 binding to Ca^{2+} as described (*34*).

To quantify the relative rates of accumulation and decay of the intracellular Ca^{2+} generated by stimulation of PAR1 and PAR4 with their peptide ligands in the presence of apyrase, the Ca^{2+} transients were fit by nonlinear regression with the equation:

$$[Ca^{2+}{}_{340/380nm}]_i = [A_o k_r/(k_d - k_r)][\exp(-k_r t) - \exp(-k_d t)] \quad (1)$$

This equation describes two consecutive and irreversible reactions (*35*) of Ca^{2+} accumulation and decay where A_o is the maximum amplitude, k_r is the first-order rate in rise of the Ca^{2+} signal, and k_d is the first-order rate of decay of the Ca^{2+} signal expressed as the ratio of fluorescence intensity, $I_{340/380}$. Best fits were performed using Kaleidagraph 3.05 until R^2 values exceeded 0.97.

Platelet Aggregation. Gel-filtered human platelets were prepared and counted as above, and adjusted to $1.5 \times 10^5/\mu$L in PBS (150 mM NaCl, 20 mM KPO_4, pH 7.5). Platelet-poor samples were prepared by centrifuging 1−2 mL of the platelet-rich sample at 16000*g* for 8 min and collecting the supernatant. Platelet aggregation was measured by light scattering using a Chronolog 560VS/490-2D aggregometer. Samples were preincubated for 5 min in the presence of 1.8 mM $CaCl_2$ prior to addition of agonist in final volumes

of 250 μL. All measurements were made at 37 °C while stirring at 900 rpm. Light scattering produced by sources other than platelet aggregation was eliminated from measured values by subtracting the scattering of a platelet-poor blank from the platelet-rich sample.

RESULTS

The PAR1- and PAR4-Induced Intracellular Ca^{2+} Transients Consist of a Spike and a Prolonged Response, Respectively. The Ca^{2+} response of platelets stimulated by thrombin is much more pronounced than the response elicited by the PAR1-specific peptide SFLLRN (*12*−*14*, *32*). The recent identification of the PAR4 thrombin receptor in human platelets (*6*, *7*) prompted us to determine whether PAR4 accounts for this additional thrombin-dependent Ca^{2+} signal. We challenged human platelets with PAR1 and PAR4 peptide ligands and compared the Ca^{2+} signals with the thrombin response. The mouse PAR4 ligand (GYPGKF) gives ~2-fold stronger PAR4 responses than the human PAR4 ligand (GYPGQV) (data not shown, and refs *9*, *10*) and was used here. Experiments were conducted in the presence of 1 mM extracellular Ca^{2+}.

We determined that the PAR1 Ca^{2+} signal has a spike-type profile and the PAR4 Ca^{2+} signal has a much longer duration profile when activated by peptide ligand or by thrombin cleavage. As shown in Figure 1A, SFLLRN induces a spike signal characterized by a rapid increase in intracellular Ca^{2+} followed by a rapid decrease back to near-baseline levels. Multiple challenges with SFLLRN peptide resulted in no further stimulation of the Ca^{2+} response, eliminating the possibility that naive PAR1 receptors are brought to the platelet surface during the time period (15 min) of the experiment.

Subsequent thrombin challenge of PAR1-desensitized platelets induces a pronounced prolonged Ca^{2+} response due to activation of non-PAR1 (i.e., PAR4) thrombin receptors (Figure 1A). This prolonged thrombin response is characterized by a slow rise in intracellular Ca^{2+} followed by a very slow reequilibration toward baseline Ca^{2+} levels. Stimulation of naive platelets with saturating thrombin (105 nM) results in a coincident spike plus prolonged response (Figure 1B). For a more quantitative evaluation of the two types of Ca^{2+} signals, we measured the integrated rise in $[Ca^{2+}]_i$ during the time of the Ca^{2+} signal, or calcium-mobilizing potency

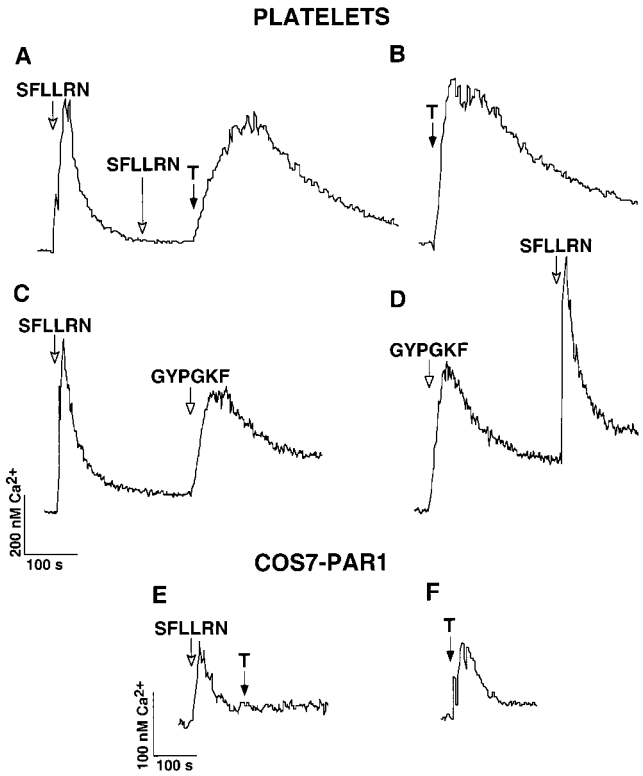

FIGURE 1: Separation of PAR1 and PAR4 Ca^{2+} responses in human platelets. Gel-filtered human platelets (A−D) and COS7 cells transiently expressing PAR1 (E and F) were loaded with 2.5 μM fura-2/AM for 30 min at 37 °C. Intracellular Ca^{2+} levels were monitored as the ratio of fluorescence excitation intensities at 340/380 nm and converted to $[Ca^{2+}]_i$ as described (*32*). Cells were challenged with 30 μM SFLLRN, 105 nM thrombin (T), and/or 1 mM GYPGKF at the indicated times.

(CMP) (*13*), for the peptide ligand and thrombin responses (Table 1). Despite similar magnitudes in the maximal $[Ca^{2+}]_i$ signals, the CMP for saturating SFLLRN (29 μM·s) is 3.5-fold less than that of thrombin (102 μM·s). The CMP of the SFLLRN spike response plus the CMP of the subsequent thrombin prolonged response is additive (29 μM·s + 74 μM·s = 103 μM·s) and equals the CMP elicited by thrombin alone (Table 1). In contrast to platelets, thrombin challenge of COS7 cells transfected with PAR1 elicits only a spike response that has the same profile and CMP as the SFLLRN-induced Ca^{2+} responses in the same cell type (Figure 1E,F).

Table 1: Properties of Platelet PAR1 and PAR4 Ca^{2+} Responses

	PAR1		PAR4		PAR1+PAR4
agonist	SFLLRN	thrombin[a]	GYPGKF	thrombin[b]	thrombin[a]
CMP[c] (μM·s)	29 ± 2		71 ± 8	74 ± 8	102 ± 9
$t_{1/2}$ activation[d] (s)		2.0 ± 1.5		145 ± 14	
EC_{50} $[\Delta Ca^{2+}]_{max}$[e]	1.8 ± 0.5 μM		800 ± 110 μM	15 ± 1 nM	7.2 ± 2 nM
EC_{50} $(\Delta Ca^{2+}/\Delta t)$[f]	9 ± 1 μM		2.7 ± 0.4 mM	125 nM	6.2 ± 0.9 nM
V_{max} $(\Delta Ca^{2+}/\Delta t)$[g] (nM·s^{-1})	75 ± 4		70 ± 10	40	62 ± 3
Ca^{2+} signal rate of decay, k_d[h] (min^{-1})	1.8 ± 0.1		0.6 ± 0.1		

[a] Thrombin response of naive platelets. [b] Thrombin response of PAR1-desensitized platelets. [c] Measurements of the Ca^{2+} signals from gel-filtered human platelets challenged with 30 μM SFLLRN, 2 mM GYPGKF, or 105 nM thrombin were performed as described in Figure 1. Calcium-mobilizing potency (CMP) is the integrated intracellular Ca^{2+} concentration in response to saturating ligand as defined by Heemskerk (*13*). [d] The $t_{1/2}$ values of thrombin receptor activation by thrombin were obtained from 3 experiments conducted on gel-purified platelets from 3 different volunteers as described in Figure 3. [e] Experiments performed as described in Figure 5B. [f] The EC_{50} for initial velocity of the Ca^{2+} flux was obtained from experiments described in Figure 5C. [g] Maximal initial velocity of Ca^{2+} flux obtained with saturating amounts of agonist (Figure 5C). [h] Apyrase-treated platelets were stimulated with 30 μM SFLLRN or 2 mM GYPGKF. The Ca^{2+} transients were fit by eq 1 (Materials and Methods) where k_d is the first-order rate of decay of the Ca^{2+} signal. For the SFLLRN-generated transient, $A_o = 2.1$,and $k_r = 11 \pm 1$ min^{-1}; for the GYPGKF-generated transient, $A_o = 4$ and $k_r = 3.0 \pm 0.1$ min^{-1}.

This is consistent with the hypothesis that the spike component of the thrombin response of platelets is derived solely from PAR1.

Next, we found that the Ca^{2+} response induced by the GYPGKF ligand mimics the prolonged portion of the thrombin response. Treatment of PAR1-desensitized or naive platelets with the GYPGKF ligand gives a robust prolonged response (Figure 1C,D). Although the GYPGKF-induced signal does not attain the full duration of the thrombin-induced PAR4 signal, the PAR4 ligand elicits up to 70% of the CMP obtained from saturating thrombin, and its response is 2.5-fold larger than the SFLLRN response (Table 1). Regardless of the order of peptide addition, the PAR4 response is prolonged, and the PAR1 response is a spike with little difference in the magnitudes of the CMP values (Figure 1C,D). We have recently identified epithelial cell lines that express PAR4 and also give prolonged Ca^{2+} signaling when stimulated with either thrombin or GYPGKF peptide.[2]

PAR1 Blocking Reagents Selectively Inhibit the Early Portion of the Platelet Ca^{2+} Response to Thrombin. To independently demonstrate that PAR1 is predominantly activated during early times after exposure to thrombin and does not directly contribute to the prolonged response, we used a polyclonal antibody (SFLLR-Ab) raised against the $S_{42}-F_{55}$ ligand region to selectively block thrombin activation of PAR1. Pretreatment of platelets with the SFLLR-Ab (37 μg/mL) eliminates the spike Ca^{2+} response without preventing the subsequent prolonged response to 1 nM thrombin (Figure 2A). Challenge of the SFLLR-Ab-pretreated platelets with 3-fold higher levels of thrombin gives a stronger prolonged response consistent with PAR4 having a lower apparent affinity for thrombin than PAR1 (*6*, *7*). Pretreatment of platelets with high levels of the PAR1 blocking antibody (220 μg/mL) results in complete and selective removal of the spike component to the Ca^{2+} response to 3 nM thrombin (Figure 2B). A control antibody (E2-Ab) raised against the first extracellular loop of PAR1, residues $S_{164}-A_{181}$, has no protective effect against the thrombin-induced spike response (data not shown). At 10 nM thrombin, the SFLLR-Ab loses ~75% of its thrombin-blocking ability on PAR1 based on residual SFLLRN activity (data not shown) and has only slight inhibitory effects on the initial velocity of the Ca^{2+} flux (Figure 2C). The same results were independently obtained using an anti-PAR1 reagent, BMS-88 (*30*). The BMS-88 compound completely blocks the response to SFLLRN and at micromolar concentrations blocks thrombin activation of PAR1. Accordingly, pretreatment of platelets with 100 μM BMS-88 removes the thrombin spike response due to blockage of PAR1 with no diminution of the prolonged response attributed to PAR4 (Figure 2D).

Kinetics of Thrombin Activation of PAR1 and PAR4 on Platelets. Next, we measured the kinetics of thrombin activation of PAR1 and PAR4 on the surface of intact platelets. Platelets were exposed to thrombin for defined periods of time, and then thrombin proteolysis was quenched by addition of hirudin. Remaining uncleaved PAR1 and PAR4 receptors were quantified by measuring the integrated Ca^{2+} response to saturating peptide ligand (Figure 3A,B).

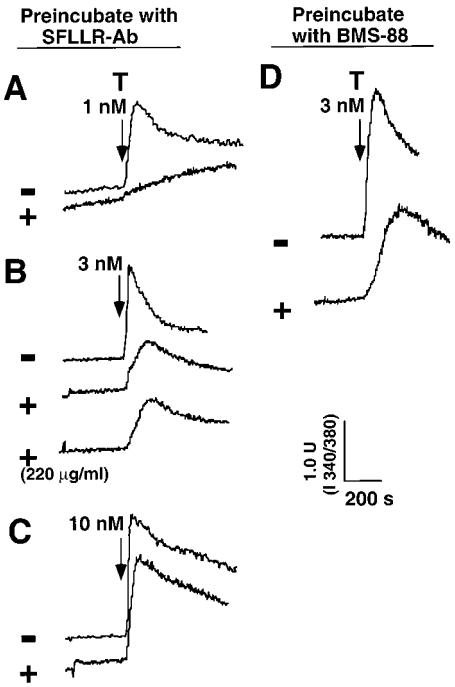

FIGURE 2: PAR1-blocking reagents preferentially remove the spike response without affecting the prolonged response of platelets challenged with thrombin. Intracellular Ca^{2+} levels were monitored as the ratio of fluorescence excitation intensities at 340/380 nm. Platelets preincubated for 250 s with either (A−C) the anti-SFLLR antibody (+) or (D) 100 μM BMS-88 (+) were challenged with 1 nM thrombin (A), 3 nM thrombin (B, D), or 10 nM thrombin (C) as indicated with the downward arrows. In (A−C), 37 μg/mL antibody (250 nM) was used during the preincubation period except for the lower trace in (B) where 220 μg/mL (1.5 μM) SFLLR-Ab was used.

The percent remaining PAR1 and PAR4 peptide responses were plotted as a function of time of hirudin quench 2−169 s after thrombin addition (Figure 3C). Thrombin activation of PAR1 is remarkably efficient with a $t_{1/2}$ of 2.0 ± 1.5 s for 10 nM thrombin (Figure 3C). During the early Ca^{2+} spike response period (0−55 s), nearly all of the PAR1 receptor population is activated by 10 nM thrombin, in agreement with measurements of direct thrombin cleavage of PAR1 expressed on RAT1 fibroblasts (*36*). After 100 s exposure to 10 nM thrombin, the residual PAR1 activity plateaus at 5−10%, which likely reflects inefficient liganding of SFLLRN to thrombin-cleaved PAR1 as has been previously observed (*37*). As predicted, the lower apparent affinity PAR4 is activated much more slowly by thrombin (Figure 3B,C). After 55 s exposure to thrombin when the spike portion of the thrombin response is nearly over, only ~30% of PAR4 is activated (Figure 3C). The $t_{1/2}$ of PAR4 activation by 10 nM thrombin is 70-fold delayed relative to the $t_{1/2}$ of PAR1 activation (Table 1).

These kinetic data also confirm that the prolonged region of the integrated Ca^{2+} response correlates with PAR4 activation and lags greatly behind PAR1 activation by thrombin. As shown in Figure 3C, the time-course of thrombin activation of PAR4 mirrors the time-integral of the cumulative thrombin Ca^{2+} response (Figure 3C, dashed line). At the $t_{1/2}$ point of 145 s of PAR4 activation by 10 nM thrombin, the cumulative thrombin response is likewise 50% complete. Conversely, at the $t_{1/2}$ point of PAR1 activation (~2 s), the cumulative Ca^{2+} response is less than 2%

[2] L. Kamath and A. Kuliopulos, unpublished data.

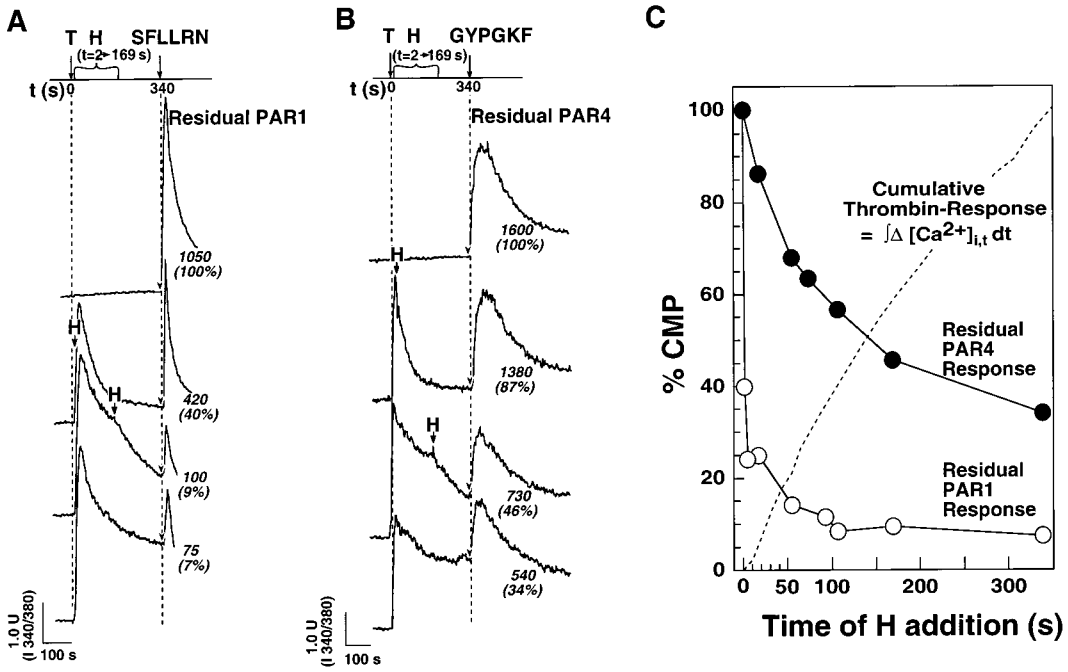

FIGURE 3: Kinetics of activation of PAR1 and PAR4 by thrombin. Platelet intracellular Ca^{2+} fluorescence was monitored as described under Materials and Methods. The experimental design is shown on top of (A, B) in schematic form. Platelets were treated with 10 nM thrombin (T) at $t = 0$ s followed by 30 μM SFLLRN (A) or 2 mM GYPGKF (B) at $t = 340$ s. Thrombin proteolysis was quenched with 0.015 unit of hirudin (H) added at indicated time points varying from 2 to 169 s. The integrated Ca^{2+} responses (CMP) for residual PAR1 (SFLLRN) or PAR4 (GYPGKF) are indicated underneath each trace and are converted to percent of the full response (% CMP). 100% CMP is the Ca^{2+} response of platelets treated solely with 30 μM SFLLRN or 2 mM GYPGKF as shown in the top traces. (C) Residual PAR1 and PAR4 responses (% CMP) of 10 nM thrombin-treated platelets (from A, B) plotted as a function of time of hirudin quench. Cumulative thrombin response, $\int\Delta[Ca^{2+}]_{i,t}\,dt$, represents the integrated Ca^{2+} responses for 10 nM thrombin over the 0−340 s time integral indicated by the dashed line.

complete. Homologous or heterologous desensitization of the total PAR1 and PAR4 responses is insignificant throughout the spike and prolonged periods. There is only 7% variability in the residual SFLLRN-dependent PAR1 activity and only 8% variability in the residual GYPGKF-PAR4 response over 15 min (data not shown). This lack of appreciable homologous or heterologous desensitization of naive PAR1 and PAR4 receptors is consistent with previous observations that the integrated Ca^{2+} response is insensitive to the rate of thrombin infusion or formation in situ (*13*).

The Prolonged Ca^{2+} Response Is Sustained by the Presence of Catalytically Active Thrombin. We determined that the PAR4-dependent prolonged portion of the platelet Ca^{2+} response requires the presence of catalytically active thrombin. Platelets were exposed to 10 nM thrombin for a variable period of time after which the thrombin activity was quenched with hirudin. When added after the immediate spike period ($t \geq 17$ s), hirudin terminates the Ca^{2+} response with a rapid decrease in intracellular Ca^{2+} back to near-baseline level (Figure 4). This demonstrates that the prolonged intracellular Ca^{2+} levels are controlled by the number of PAR4 receptors that are being actively cleaved at any given time. For instance, when 10 nM thrombin was quenched after a long exposure time of 169 s (indicated by H_3 in Figure 4), the intracellular Ca^{2+} level quickly receded. At the 169 s time point, PAR1 has already been completely activated and desensitized, but 50% of the PAR4 activity remains (Figure 3B). Thus, we can conclude that the prolonged Ca^{2+} response is largely sustained by continuous cleavage of PAR4 thrombin receptors.

Kinetics of the PAR1 and PAR4 Ca^{2+} Fluxes. The initial velocities of the $[Ca^{2+}]_i$ flux in response to various thrombin

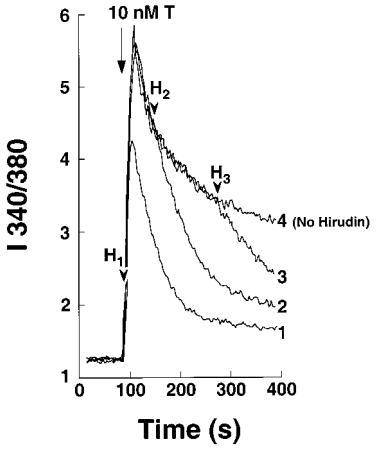

FIGURE 4: The prolonged Ca^{2+} response requires the presence of catalytically active thrombin. Gel-filtered platelets were treated with 10 nM thrombin (T) at $t = 0$ s, and intracellular Ca^{2+} was monitored by fura-2/AM fluorescence as described under Materials and Methods. Thrombin proteolysis was quenched with 0.015 unit of hirudin (H) as indicated with arrowheads at $H_1 = 2$ s (trace 1), $H_2 = 55$ s (trace 2), and $H_3 = 169$ s (trace 3). Trace 4 is a full thrombin response.

concentrations were determined for PAR1 and PAR4. The initial velocities of the Ca^{2+} flux due to thrombin cleavage of PAR4 were obtained by removing the PAR1 contribution with the PAR1-blocking antibody, by treatment with BMS-88, or by prior desensitization with SFLLRN. The $\Delta[Ca^{2+}]$ EC_{50} for thrombin cleavage of PAR4 (15 nM) in PAR1-desensitized platelets is only 2-fold weaker than thrombin cleavage of PAR1+PAR4 (7.2 nM) in naive platelets (Figure 5B, Table 1). Remarkably, the initial velocities of Ca^{2+} influx for the PAR4 prolonged response in PAR1-desensitized

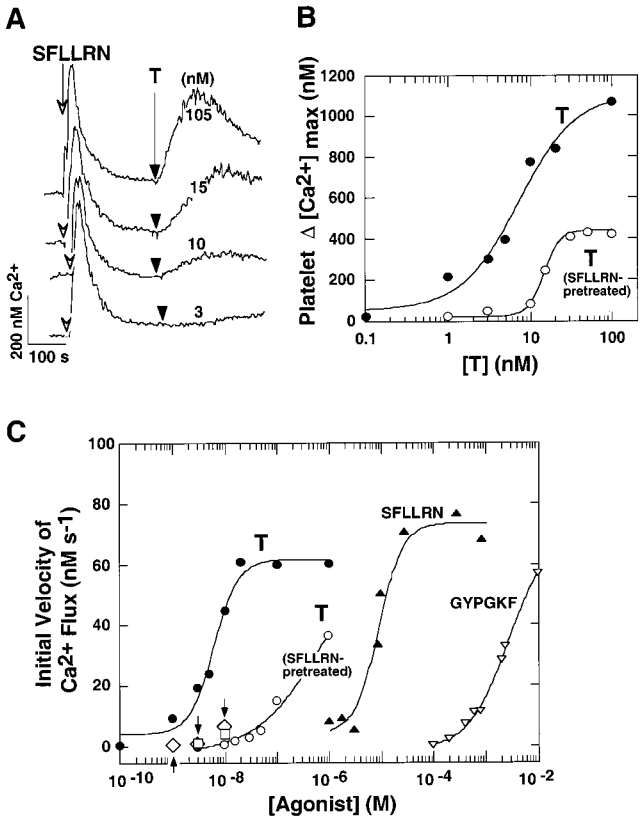

FIGURE 5: Thrombin activates PAR4 20−70-fold more slowly than PAR1. Platelet $[Ca^{2+}]_i$ was monitored by fluorescence as previously described. (A) Platelets were first treated with 30 μM SFLLRN and then with the indicated concentrations of thrombin (3−105 nM). (B) Peak intracellular Ca^{2+} for naive platelets (●) and platelets pretreated with 30 μM SFLLRN (○) plotted as a function of thrombin concentration. (C) Initial velocities of the thrombin-dependent Ca^{2+} flux in untreated platelets (●), or platelets pretreated with 30 μM SFLLRN (○). The arrows indicate the initial velocities of Ca^{2+} flux from platelets pretreated with 100 μM BMS-88 (□) or 37 μg/mL anti-SFLLR Ab (◇) and then challenged with 1−10 nM thrombin. Also shown are the initial velocities of Ca^{2+} flux from platelets stimulated with SFLLRN (▲) and GYPGKF (▽) plotted as a function of agonist concentration.

platelets are 20−70-fold slower than the PAR1 spike response upon treatment of naive platelets with 1−30 nM thrombin (Figure 5A,C). Because of this large difference in rates of activation, we did not correct for the contribution of PAR4 to the initial velocity of Ca^{2+} flux from thrombin-activated PAR1 using naive platelets. The thrombin EC_{50} for the initial velocities of Ca^{2+} influx was 6.2 nM for PAR1 and ≥125 nM for PAR4 (Figure 5C). In other assays (data not shown), we determined that 30 μM SFLLRN peptide does not inhibit thrombin cleavage of a soluble PAR1 exodomain (*32*), thereby ruling out that these profound slope effects are due to SFLLRN acting as a direct thrombin inhibitor. Moreover, similar disparities in the initial velocities of Ca^{2+} flux induced by PAR1 and PAR4 were independently obtained using the PAR1-blocking antibody or the BMS-88 compound. In platelets pretreated with either SFLLR-Ab or BMS-88, the PAR4 Ca^{2+} flux velocity was 20−40-fold slower than the thrombin-dependent PAR1 initial velocity at 1−3 nM thrombin concentrations (Figure 5C, diamonds and squares, respectively).

The initial velocities of the PAR1- and PAR4-dependent Ca^{2+} fluxes did not reach a maximum until high levels (>20 nM) of thrombin were used. Therefore, the rate-determining step(s) of the initial Ca^{2+} signal is (are) directly dependent on thrombin association and cleavage of the PAR1/4 receptors and is (are) not limited by the intracellular Ca^{2+} signaling components until saturation of the PARs is reached. Once saturated with thrombin, the maximal initial velocities of Ca^{2+} fluxes (V_{max}) for PAR1 and PAR4 reach the range of 40−60 nM s^{-1}. The V_{max} values are similar regardless of whether PAR1 and PAR4 are activated by saturating peptide ligand or by thrombin although much more peptide ligand is needed to fully activate the PARs (Figure 5C). This implies that the intracellularly located G proteins that activate Ca^{2+} signaling do not distinguish between peptide-activated receptor and thrombin-cleaved receptor.

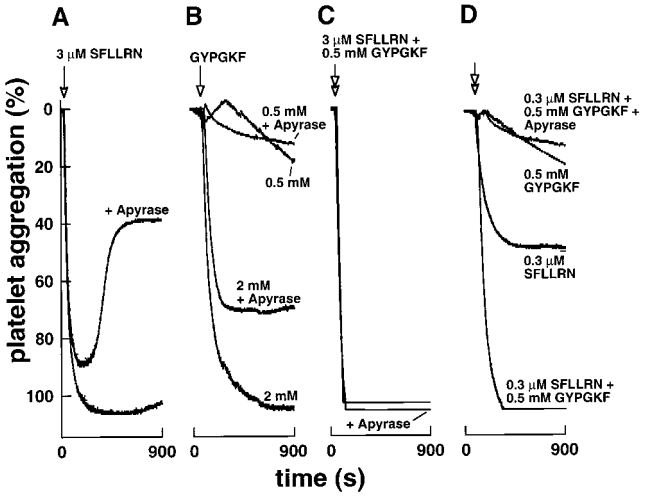

FIGURE 6: Contribution of secondary ADP autocrine stimulation to PAR1- and PAR4-dependent platelet aggregation. Gel-filtered human platelets were prepared as described under Materials and Methods. Platelet aggregation was monitored by percent transmittance of stirred platelets at 37 °C. Platelets were preincubated for 2 min with 0.2 unit/mL final concentration apyrase where indicated and then stimulated with SFLLRN and/or GYPGKF.

Synergism of the PAR1, PAR4, and Secondary ADP Autocrine Stimulus-Response to Platelet Aggregation. We also examined the relative contributions of PAR1, PAR4, and secondary ADP autocrine stimulation to platelet aggregation. The dense granules contain large amounts of ATP/ADP which are nearly completely released within 10−30 s during platelet activation by 10−30 nM thrombin (data not shown and ref *9*). The secreted ADP activates ADP receptors to further augment the aggregation process (*38*). As shown in Figure 6A, 3 μM SFLLRN causes full and irreversible platelet aggregation. In the presence of the ADP-degrading enzyme apyrase, aggregation induced by 3 μM SFLLRN becomes partially reversible. More robust stimulation of PAR1 with >10 μM SFLLRN, however, is sufficient to cause irreversible platelet aggregation in the presence of apyrase (data not shown). Addition of 2 mM GYPGKF to platelets also causes full and irreversible platelet aggregation (Figure 6B). Lower amounts of GYPGKF (0.5 mM) cause full shape change (7% negative deflection in light transmittance) but achieve only partial platelet aggregation. Addition of apyrase inhibits the extent of GYPGKF-induced platelet aggregation but does not reverse the aggregation process.

Contributions from PAR4 can also act synergistically with PAR1 at subthreshold levels of either receptor agonist to promote platelet aggregation. Addition of subthreshold

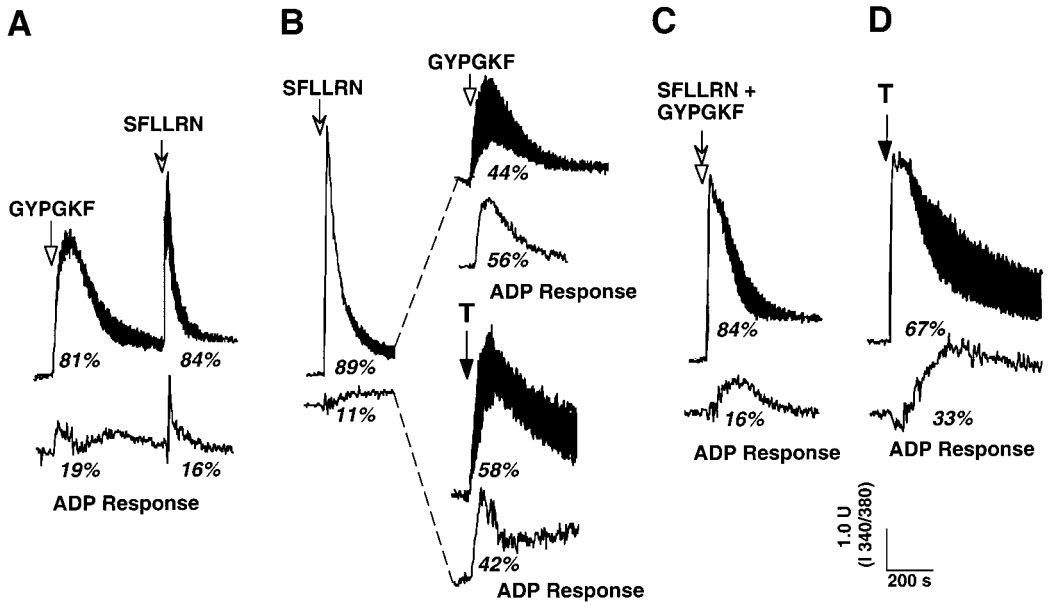

FIGURE 7: Contribution of secondary ADP autocrine stimulation to the PAR1 and PAR4 Ca^{2+} responses in real time. Ca^{2+} fluorescence measurements were performed on gel-filtered platelets challenged with 2 mM GYPGKF, 30 μM SFLLRN, or 20 nM thrombin (T) in the presence or absence (top-shaded traces) of 0.2 units/mL of apyrase. The bottom trace (ADP response) in each series was obtained by subtracting the transient generated in the presence of apyrase from the corresponding transient generated in the absence of apyrase. The integrated Ca^{2+} responses (CMP) for the individual treatments are converted to % CMP relative to the full Ca^{2+} response in the absence of apyrase and are shown under each trace.

amounts of GYPGKF (0.5 mM) rescues the reversible platelet aggregation defect elicited by apyrase plus 3 μM SFLLRN (Figure 6C), and simultaneous addition of subthreshold SFLLRN (0.3 μM) and subthreshold GYPGKF (0.5 mM) is able to effect full, irreversible, platelet aggregation (Figure 6D). This is true, however, only with the assistance from secondary ADP stimulation. Together these data demonstrate that strong signals from PAR1 or PAR4 can cause full and irreversible platelet aggregation, but at subthreshold PAR1/4 activation, irreversible platelet aggregation requires the assistance of secondary ADP autocrine stimulation.

Efficient ADP Autocrine Ca^{2+} Stimulation Requires Sequential Activation of PAR1 and PAR4. We assessed the contribution of ADP autocrine stimulation to the PAR1- and PAR4-dependent Ca^{2+} fluxes in real-time. Most surprisingly, we found that PAR4 contributes to the majority of the secondary ADP Ca^{2+} effect induced by thrombin and that this effect is dependent on prior PAR1 stimulation. As shown in Figure 7A,B, challenge of naive platelets with PAR4 or PAR1 peptide ligands causes modest ADP autocrine stimulation of platelet intracellular Ca^{2+}. This is shown by recording the platelet Ca^{2+} fluxes in the presence or absence of apyrase; hence, addition of apyrase causes a drop of 19% in the GYPGKF response (Figure 7A) and a drop of 11% in the SFLLRN response (Figure 7B). The Ca^{2+} transient contributed by ADP (ADP responses of Figure 7) can then be revealed by subtracting the transient obtained from apyrase-treated platelets from the transient obtained from untreated platelets stimulated with the same agonist(s). Addition of SFLLRN after prior stimulation of PAR4 with the GYPGKF ligand elicits only a 16% ADP effect on the CMP with no effect on the initial velocity of the Ca^{2+} flux (Figure 7A). In marked contrast, addition of GYPGKF after prior stimulation of PAR1 with SFLLRN shows a large ADP effect both on the magnitude of the CMP (56%) and on the initial velocity of the Ca^{2+} flux elicited by PAR4 (Figure 7B). Similar results are seen upon thrombin activation of PAR4 in platelets prestimulated with the PAR1 peptide ligand (Figure 7B). Simultaneous artificial stimulation of PAR1 and PAR4 by co-addition of SFLLRN and GYPGKF does not elicit a significant ADP effect (Figure 7C). Sequential activation of PAR1 and PAR4 by addition of 20 nM thrombin, however, gives a progressively stronger ADP effect that coincides with the PAR4-dependent portion of the Ca^{2+} transient (Figure 7D). Similar results were obtained using thrombin concentrations from 10 to 1000 nM. These data demonstrate that PAR4 is much more efficient in eliciting the secondary ADP Ca^{2+} effect after prior stimulation of PAR1 with either SFLLRN or thrombin.

It is noteworthy that the SFLLRN- and GYPGKF-induced Ca^{2+} profiles remain distinctly spiked and prolonged, respectively, even upon removal of the ADP effect with apyrase. Also evident in Figure 7, the time course of Ca^{2+} decay was slower for PAR4 than for PAR1 responses. This was true even in the presence of apyrase and thus cannot be attributed to PAR4's stronger ADP effect. To quantify this kinetic difference, Ca^{2+} transients were fitted with eq 1 (see Materials and Methods) which describes an irreversible, two-step accumulation and decay process. The decay time constants from these fits (see Table 1) indicate that in the presence of apyrase SFLLRN-induced Ca^{2+} responses decay 3-fold faster than do GYPGKF-induced responses. Furthermore, this 3-fold difference in rate-of-decay is independent of the concentration of the stimulant (0.1−2.4 mM GYPGKF, 1−30 μM SFLLRN). This result suggests an intrinsic difference in the rate of PAR1 and PAR4 desensitization.

The PAR1 and PAR4 Responses Are Comprised of Parallel Intracellular and Extracellular Ca^{2+} Fluxes. Last, we conducted experiments that measured the relative contributions of intracellular Ca^{2+} store-release versus extracellular Ca^{2+} influx resulting from inputs from PAR1 and PAR4.

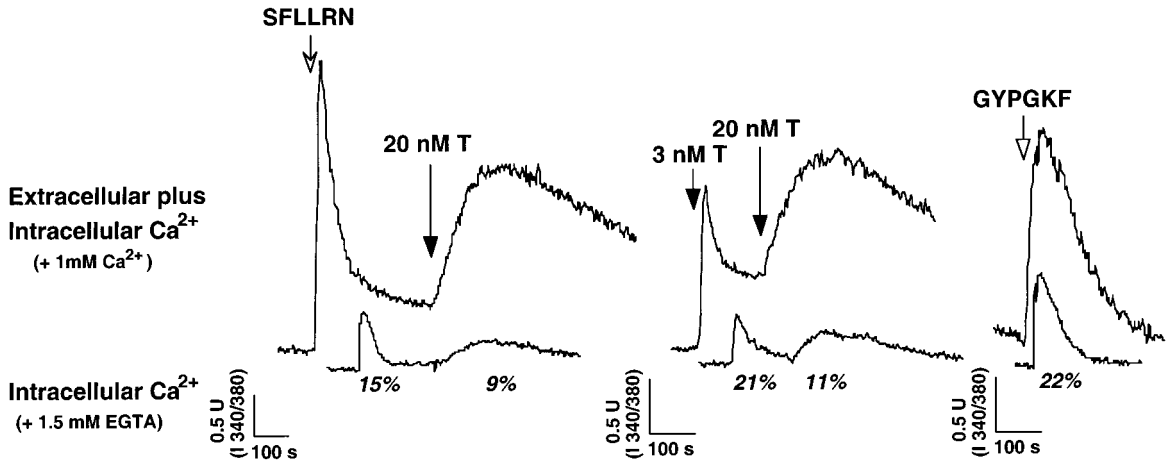

FIGURE 8: The PAR1 and PAR4 responses are comprised of parallel intracellular and extracellular Ca^{2+} fluxes. Ca^{2+} measurements are made in the presence of 1 mM Ca^{2+} (upper traces) or 1.5 mM EGTA (lower traces). Gel-purified platelets were stimulated with 30 μM SFLLRN, 2 mM GYPGKF, or 3−20 nM thrombin as indicated. The integrated Ca^{2+} responses (CMP) for the individual treatments are converted to percentage of intracellular Ca^{2+} store-release relative to the full Ca^{2+} response in the presence of extracellular Ca^{2+} and are shown under each trace.

The contribution of intracellular Ca^{2+} store-release to the intracellular Ca^{2+} flux was measured by incubating the platelets in Ca^{2+}-free media in the presence of EGTA to remove any residual extracellular Ca^{2+}. As shown in Figure 8, the majority of the Ca^{2+} flux elicited by activated PAR1 and PAR4 is due to influx through the plasma membrane Ca^{2+} channels. For both receptors, however, a component from internal stores was evident regardless of whether PAR1 or PAR4 was stimulated by peptide or by thrombin. Intracellular Ca^{2+} store-release contributes 9−22% of the total cumulative Ca^{2+} response to PAR1 and PAR4. Thus, ~80−90% of the cumulative Ca^{2+} response is due to Ca^{2+} influx regardless of the mode of activation. Moreover, both receptors strongly activate plasma membrane Ca^{2+} channels despite the 2.5-fold difference in total integrated Ca^{2+} responses.

The contribution of outside-in signaling from the αIIbβ3 integrin was determined by incubating the platelets with 1 mM RGDS, a peptide which prevents fibrinogen binding to αIIbβ3. The CMP values of RGDS-treated versus untreated platelets differed by less than 3% upon stimulation with 10 nM thrombin even though the RGDS peptide inhibited 80−90% of platelet aggregation (data not shown). Therefore, using nonstirred, gel-filtered platelets, we did not detect any significant contribution from αIIbβ3 to the Ca^{2+} transients generated by thrombin.

DISCUSSION

Mouse genetic experiments have elegantly identified the presence of multiple thrombin receptors in platelets (*7*, *39*). A theme is now emerging that platelets have dual thrombin-activated receptors—a high-affinity receptor such as PAR1 or PAR3 and a lower apparent affinity PAR4 receptor. Indeed, PAR1 and PAR4 account for nearly all of the actions of thrombin in activating human platelets. Addition of blocking reagents directed against PAR1 or PAR4 showed that each is capable of activating platelets (*9*), thus arguing that the dual receptors provide apparent functional redundancy. The studies presented here, however, reveal striking differences in the signaling properties of PAR1 and PAR4. This biphasic activation of PAR1 and PAR4 on the outside of the platelet in turn causes biphasic Ca^{2+} signals inside the platelet. We propose a sequential thrombin receptor activation mechanism that gives rise to the spike and prolonged intracellular transients in platelets (Figure 9).

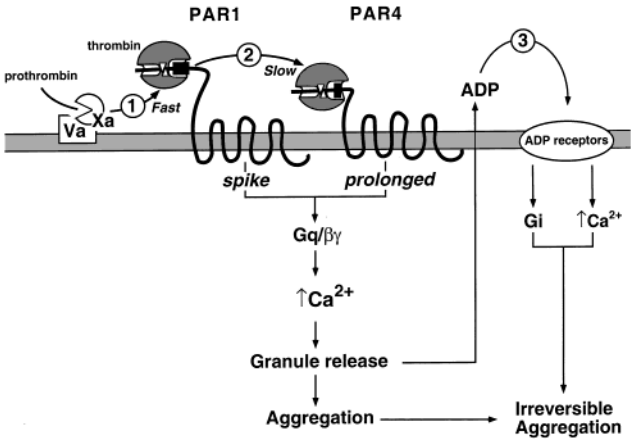

FIGURE 9: Sequential thrombin receptor activation mechanism. The sequential PAR1 and PAR4 thrombin receptor activation mechanism regulates the shape and the duration of the spike and prolonged Ca^{2+} signals. During blood coagulation, the Xa/Va complex generates thrombin that first activates the high-affinity PAR1 [1] and then dissociates and binds to the lower apparent affinity PAR4 receptor [2]. Cleavage of PAR1 and PAR4 by thrombin generates the biphasic PAR1-spike and PAR4-prolonged Ca^{2+} transients via $G_q/\beta\gamma$ and PLCβ isoforms. The high intracellular Ca^{2+} levels trigger release of ADP from the dense granules. Activated ADP receptors [3] further augment the Ca^{2+} response and progression to irreversible aggregation. The plasma membrane ADP receptors include $P2Y_1$ (which couples to G_q), $P2Y/P2T_{AC}$ (which couples to G_{i2}), and $P2X_1$ (which is a ligand-gated Ca^{2+} channel) (*38*). The closed boxes on PAR1 and PAR4 represent high- and low-affinity hirudin-like sequences, respectively, that bind to exosite I on thrombin.

Sequential Activation Mechanism. Initially, lower concentrations of thrombin preferentially cleave the high apparent affinity PAR1 and rapidly stimulate a Ca^{2+} signal that has a distinct spike profile. PAR1 produces a relatively small secondary Ca^{2+} effect from secreted ADP. The presence of continuously higher concentrations of thrombin generated in situ by the Xa/Va complex during active blood clotting (*40*) activates PAR4 to produce sustained high intracellular Ca^{2+} levels. Approximately 50% of the prolonged Ca^{2+}

response derives from PAR4-dependent secondary ADP autocrine stimulation. Interruption of the supply of catalytically active thrombin during this late phase causes a precipitous drop in the intracellular Ca^{2+} levels that could adversely affect late Ca^{2+}-dependent processes which promote irreversible platelet aggregation. Indeed, it has long been recognized that quench of thrombin-activated platelets with hirudin after less than 20% aggregation has occurred results in dissociation of platelet−platelet contacts and reversal of aggregation (*41*).

Since all platelet thrombin receptors contain purported hirudin-like binding sites for thrombin (*42*), why is PAR1 rapidly activated whereas PAR4 is activated over a much longer time period and leads to the observed prolonged Ca^{2+} signal? We will consider two possible contributing factors: (i) PAR1 has an intrinsically higher affinity for thrombin than does PAR4. Coughlin and colleagues (*7*) have shown that mPAR4 has a 40-fold poorer EC_{50} for thrombin than mPAR1 using a frog egg system. Likewise, hPAR4 has a relatively poor EC_{50} for thrombin (10−75 nM) when expressed in COS7 fibroblasts (*6*). We also observe a similar 20-fold difference in EC_{50} values for the initial velocities of Ca^{2+} flux for PAR1 versus PAR4 (Figure 5C). Therefore, it is possible that thrombin binds first to the higher affinity PAR1 due to a favorable association constant, K_a,[3] and then dissociates to bind and cleave the PAR4 receptors which have a lower K_a. (ii) An accessory protein such as GPIb aids in thrombin cleavage of PAR1 and/or conversely slows down the cleavage of PAR4. Although well accepted as a bona fide thrombin-binding protein with 10^8 M^{-1} affinity, the role of GPIb as a positive effector of thrombin activation of platelets remains controversial (*42*−*45*). GPIb may even be a negative regulator of thrombin activation of platelets (*46*) and could contribute to the slow cleavage or intramolecular activation of PAR4. Another candidate thrombin-sequestering protein is GPV. Deletion of GPV causes murine platelets to become hyper-responsive to thrombin and decreases the bleeding time, suggesting a possible negative role for GPV in thrombin activation of platelet receptors (*47*).

Distinct Ca^{2+} Signaling from PAR1 versus PAR4. The two subtypes of platelet thrombin receptors stimulate intracellular Ca^{2+} release and Ca^{2+} influx in parallel. The early Ca^{2+} spike and the prolonged Ca^{2+} transient are comprised primarily of Ca^{2+} entry from outside the cell with a 10−20% contribution from internal Ca^{2+} release. Our results suggest that the G_q-dependent mechanism that controls intracellular Ca^{2+} store-release (*16*) is strongly coupled with Ca^{2+} influx for both receptors. However, there are four differences in the quality of the Ca^{2+} signal induced by the two types of thrombin receptors. First, there is a 20−70-fold disparity in the initial velocities of Ca^{2+} flux due to much slower thrombin-dependent activation of PAR4 relative to PAR1. This disparity is not seen at saturating levels of peptide ligands. Therefore, PAR1 and PAR4 have similar capabilities in eliciting maximal rates of Ca^{2+} influx, and it is extracellular thrombin activation of PAR4 that is rate-limiting rather than an internal event such as coupling with G protein (Figure 5). Second, the input signal from PAR1 reaches its maximum within 10−20 s whereas the input signal from PAR4 reaches its maximum (100−150 s) significantly later. Third, there are striking differences in the time needed to regain baseline levels (∼75 nM) of intracellular Ca^{2+}. Even in the absence of the secondary ADP effect, the SFLLRN-stimulated PAR1 Ca^{2+} signal decays with a rate that is 3-fold faster than the GYPGKF-stimulated PAR4 Ca^{2+} signal. This 3-fold difference in decay rate of the net intracellular Ca^{2+} concentration could simply be due to dissimilar rates of desensitization of PAR1 and PAR4, i.e., differential receptor phosphorylation (*32*, *48*). Alternatively, PAR4 could more strongly activate other second messengers that may control the late phase of Ca^{2+} influx (*11*, *19*, *21*, *49*). Fourth, up to 50% of the PAR4 Ca^{2+} signal is due to secondary ADP autocrine stimulation. Interestingly, this strong ADP effect requires prior stimulation of PAR1 either artificially with the SFLLRN ligand or by sequential cleavage with thrombin. Activated PAR1 produces a minor ADP autocrine Ca^{2+} response that is not affected by prior stimulation of PAR4.

Is the heightened ADP−Ca^{2+} response from activated PAR4 simply due to granule secretion? Other studies (*50*, *51*) have shown that PAR1 activation by the SFLLRN peptide is 85−100% as efficient as activation by thrombin in stimulating release of dense granules contents. Therefore, PAR1 is able to activate full granule secretion. In another study, Mazzucato et al. (*45*) showed that pretreatment of platelets with an anti-PAR1 antibody diminishes thrombin-dependent ATP release by 80%. This is consistent with our observations that the majority of granule secretion is due to PAR1.[4] Moreover, they also showed that a marker of α-granule release, P-selectin, reached its maximum expression within 20 s upon stimulation with low concentrations of thrombin (1 nM). This early secretion event coincides with the PAR1 Ca^{2+} response and precedes the strong ADP−Ca^{2+} response from activated PAR4 (Figure 7). It is therefore highly unlikely that the enhanced PAR4 ADP−Ca^{2+} response is simply due to granule release. Instead, it appears that PAR4 potentiates the ADP response by an as yet unidentified mechanism. Presently, we are examining the intricate interrelationships of PAR1, PAR4, and ADP receptors in order to define their respective inputs to calcium signaling and platelet physiology. Intriguingly, as noted above, we found that the ADP contribution to the Ca^{2+} response is greatly affected by the order of activation of the thrombin receptors. This unique feature of the PAR4 receptor attests to a distinct role of PAR4 in platelet signaling. Much like the anti-ADP receptor drugs clopidogrel and ticlopidine (*52*), therapeutics targeted against PAR4 could be beneficial as adjuvant treatment for patients at high risk for thrombotic events and not in cases where rapid anti-platelet effects are necessary.

[3] S. Jacques and A. Kuliopulos, unpublished data.
[4] L. Kamath and A. Kuliopulos, unpublished data.

ACKNOWLEDGMENT

We thank David Potter, Dan Cox, Suzanne Jacques, and Steve Swift for critically reviewing the manuscript and for many thoughtful discussions.

REFERENCES

1. Coughlin, S. R. (1994) *Proc. Natl. Acad. Sci. U.S.A. 91*, 9200−9202.
2. Vu, T.-K. H., Hung, D. T., Wheaton, V. I., and Coughlin, S. R. (1991a) *Cell 64*, 1057−1068.
3. Rasmussen, U. B., Vouret-Craviari, V., Jallat, S., Schlesinger, Y., Pages, G., Pavirani, A., Lecocq, J.-P., Pouyssegur, J., and Obberghen-Schilling, E. V. (1991) *FEBS Lett. 288*, 123−128.

4. Nystedt, S., Emilsson, K., Wahlestedt, C., and Sundelin, J. (1994) *Proc. Natl. Acad. Sci. U.S.A. 91*, 9208−9212.
5. Ishihara, H., Connolly, A. J., Zeng, D., Kahn, M. L., Zheng, Y. W., Timmons, C., Tram, T., and Coughlin, S. R. (1997) *Nature 386*, 502−506.
6. Xu, W.-F., Andersen, H., Whitmore, T. E., Presnell, S. R., Yee, D. P., Ching, A., Gilbert, T., Davie, E. W., and Foster, D. C. (1998) *Proc. Natl. Acad. Sci. U.S.A. 95*, 6642−6646.
7. Kahn, M. L., Zheng, Y.-W., Huang, W., Bigornia, V., Zheng, D., Moff, S., Farese, R. V., Tam, C., and Coughlin, S. R. (1998) *Nature 394*, 690−694.
8. Ishihara, H., Zeng, D., Connolly, A. J., Tam, C., and Coughlin, S. R. (1998) *Blood 91*, 4152−4157.
9. Kahn, M. L., Nakanishi-Matsui, M., Shapiro, M. J., Ishihara, H., and Coughlin, S. R. (1999) *J. Clin. Invest. 103*, 879−887.
10. Anderson, H., Greenberg, D. L., Fujikawa, K., Xu, W., Chung, D. W., & Davie, E. W. (1999) *Proc. Natl. Acad. Sci. U.S.A. 96*, 11189−11193.
11. Lau, L.-F., Pumiglia, K., Cote, Y. P., and Feinstein, M. B. (1994) *Biochem. J. 303*, 391−400.
12. Lasne, D., Donato, J., Falet, H., and Rendu, F. (1995) *Thromb. Haemostasis 74*, 1323−1328.
13. Heemskerk, J. W. M., Feijge, M. A. H., Henneman, L., Rosing, J., and Hemker, H. C. (1997) *Eur. J. Biochem. 249*, 547−555.
14. Aoki, T., Tomiyama, Y., Honda, S., Senzaki, K., Tanaka, A., Okubo, M., Takahashi, F., Takasugi, H., and Seki, J. (1998) *Thromb. Haemostasis 79*, 1184−1190.
15. Yang, X., Sun, L., Ghosh, S., and Rao, A. K. (1996) *Blood 88*, 1676−1683.
16. Offermanns, S., Toombs, C. F., Hu, Y.-H., and Simon, M. I. (1997) *Nature 389*, 183−186.
17. Gabbeta, J., Yang, X., Kowalska, M. A., Sun, L., Dhanasekaran, N., and Rao, A. K. (1997) *Proc. Natl. Acad. Sci. U.S.A. 94*, 8750−8755.
18. Rink, T. J., and Sage, S. O. (1990) *Annu. Rev. Physiol. 52*, 431−449.
19. Sage, S. O., Merritt, J. E., Hallam, T. J., and Rink, T. J. (1989) *Biochem. J. 258*, 923−926.
20. Hashimoto, Y., Ogihara, A., Nakanishi, S., Matsuda, Y., Kurokawa, K., and Nonomura, Y. (1992) *J. Biol. Chem. 267*, 17078−17081.
21. Lu, P.-J., Hsu, A.-L., Wang, D.-S., and Chen, C.-S. (1998) *Biochemistry 37*, 9776−9783.
22. Clark, E. A., and Brugge, J. S. (1995) *Science 268*, 233−239.
23. Law, D. A., DeGuzman, F. R., Heiser, R., Ministri-Madrid, K., Killeen, M., and Phillips, D. R. (1999) *Nature 401*, 808−811.
24. Lind, S. E., Janmey, P. A., Chaponnier, C., Herbert, T. J., and Stossel, T. P. (1987) *J. Cell Biol. 105*, 833−842.
25. Shattil, S. J., Ginsberg, M. H., and Brugge, J. S. (1994) *Curr. Opin. Cell Biol. 6*, 695−704.
26. Potter, D., Tirnauer, J. S., Janssen, R., Croall, D. E., Hughes, C. N., Fiacco, K. A., Mier, J. W., Maki, M., and Herman, I. M. (1998) *J. Cell Biol. 141*, 647−662.
27. Croce, K., Flaumenhaft, R., Rivers, M., Furie, B., Furie, B. C., Herman, I. M., and Potter, D. A. (1999) *J. Biol. Chem. 274*, 36321−36327.
28. Du, X., Saido, T. C., Tsubuki, S., Indig, F. E., Williams, M. J., and Ginsberg, M. H. (1995) *J. Biol. Chem. 270*, 26146−26151.
29. Kovacsovics, T. J., and Hartwig, J. H. (1996) *Blood 87*, 618−629.
30. Bernatowicz, M. S., Klimas, C. E., Hartl, K. S., Peluso, M., Allegretto, N. J., and Seiler, S. M. (1996) *J. Med. Chem. 39*, 4879−4887.
31. Kuliopulos, A., Nelson, N. P., Yamada, M., Walsh, C. T., Furie, B., Furie, B. C., and Roth, D. A. (1994) *J. Biol. Chem. 269*, 21364−21370.
32. Kuliopulos, A., Covic, L., Seeley, S. K., Sheridan, P. J., Helin, J., and Costello, C. E. (1999) *Biochemistry 38*, 4572−4585.
33. Hsu-Lin, S., Berman, C. L., Furie, B. C., August, D., and Furie, B. (1984) *J. Biol. Chem. 259*, 9121−9126.
34. Grynkiewicz, G., Poenie, M., and Tsien, R. Y. (1985) *J. Biol. Chem. 260*, 3440−3450.
35. Fersht, A. (1985) in *Enzyme Structure and Mechanism*, pp 132−134, W. H. Freeman and Company, New York.
36. Ishii, K., Hein, L., Kobilka, B., and Coughlin, S. R. (1993) *J. Biol. Chem. 268*, 9780−9786.
37. Hammes, S. R., and Coughlin, S. R. (1999) *Biochemistry 38*, 2486-2493.
38. Cattaneo, M., and Gachet, C. (1999) *Arterioscler. Thromb. Vasc. Biol. 19*, 2281−2285.
39. Connolly, A. J., Ishihara, H., Kahn, M. L., Farese, R. V., and Coughlin, S. R. (1996) *Nature 381*, 516−519.
40. Rand, M. D., Lock, J. B., Veer, C. V., Gaffney, D. P., and Mann, K. G. (1996) *Blood 88*, 3432−3445.
41. Holmsen, H., Dangelmaier, C. A., and Holmsen, H.-K. (1981) *J. Biol. Chem. 256*, 9393−9396.
42. Hayes, K. L., and Tracy, P. B. (1999) *J. Biol. Chem. 274*, 972−980.
43. Greco, N. J., Tandon, N. N., Jones, G. D., Kornhauser, R., Jackson, B., Yamamoto, N., Tanoue, K., and Jamieson, G. A. (1996a) *Biochemistry 35*, 906−914.
44. Liu, L., Freedman, J., Hornstein, A., Fenton, J. W., Song, Y., and Ofosu, F. A. (1997) *J. Biol. Chem. 272*, 1997−2004.
45. Mazzucato, M., Marco, L. D., Masotti, A., Pradella, P., Bahou, W. F., and Ruggeri, Z. M. (1998) *J. Biol. Chem. 273*, 1880−1887.
46. Leong, L., Hendrickson, R. A., Kermode, J. C., Rittenhouse, S. E., and Tracy, P. B. (1992) *Biochemistry 31*, 2567−2576.
47. Ramakrishnan, V., Reeves, P. S., DeGuzman, F., Deshpande, U., Ministri-Madrid, K., DuBridge, R. B., and Phillips, D. R. (1999) *Proc. Natl. Acad. Sci. U.S.A. 96*, 13336−13341.
48. Hammes, S. R., Shapiro, M. J., and Coughlin, S. R. (1999) *Biochemistry 38*, 9308−9316.
49. Banfic, H., Downes, P., and Rittenhouse, S. E. (1998) *J. Biol. Chem. 273*, 11630−11637.
50. Kinlough-Rathbone, R. L., Perry, D. W., Guccione, M. A., Rand, M. L., and Packham, M. A. (1993) *Thromb. Haemostasis 70*, 1019−1023.
51. Kinlough-Rathbone, R. L., Perry, D. W., and Packham, M. A. (1995) *Thromb. Haemostasis 73*, 122−5.
52. Harker, L. A. (1998) *Cerebrovasc. Dis. 8*, 8−18.

BI9927078